

Evidence for Nonlinear X-ray Variability from the Broad-line Radio Galaxy 3C 390.3

Karen M. Leighly¹

Cosmic Radiation Laboratory, RIKEN, Hirosawa 2-1, Wako-shi, Saitama 351, Japan,
leighly@postman.riken.go.jp

Paul T. O'Brien

Department of Physics & Astronomy, University of Leicester, University Road, Leicester,
LE1 7RH, U.K., pto@star.le.ac.uk

ABSTRACT

We present analysis of the light curve from the *ROSAT* HRI monitoring observations of the broad-line radio galaxy 3C 390.3. Observed every three days for about 9 months, this is the first well sampled X-ray light curve on these time scales. The flares and quiescent periods in the light curve suggest that the variability is nonlinear, and a statistical test yields a detection with $\gtrsim 6\sigma$ confidence. The structure function has a steep slope ~ 0.7 , while the periodogram is much steeper with a slope ~ 2.6 , with the difference partially due to a linear trend in the data. The non-stationary character of the light curve could be evidence that the variability power spectrum has not turned over to low frequencies, or it could be an essential part of the nonlinear process. Evidence for X-ray reprocessing suggests that the X-ray emission is not from the compact radio jet, and the reduced variability before and after flares suggests there cannot be two components contributing to the X-ray short term variability. Thus, these results cannot be explained easily by simple models for AGN variability, including shot noise which may be associated with flares in disk-corona models or active regions on a rotating disk, because in those models the events are independent and the variability is therefore linear. The character of the variability is similar to that seen in Cygnus X-1, which has been explained by a reservoir or self-organized criticality model. Inherently nonlinear, this model can reproduce the reduced variability before and after large flares and the steep PDS seen generally from AGN. The 3C 390.3 light curve presented here is the first support for such models to explain AGN variability on intermediate time scales from a few days to months.

Subject headings: galaxies: individual (3C 390.3) – X-rays: galaxies – galaxies: active

¹Current address: Columbia Astrophysics Laboratory, 538 West 120th Street, New York, NY 10025, USA,
leighly@ulisse.phys.columbia.edu

1. Introduction

X-ray variability has been observed in active galaxies (AGN) for two decades, but the origin of the variability is comparatively poorly understood. So far, the *EXOSAT* long observations have provided the most constraining results on AGN variability. On time scales < 3 days, the power density spectrum (PDS) can be described with a power law of slope $s > 1$ ($P(f) \propto f^{-s}$). The index clusters around $s = 1.55$ over a large range of luminosity; further, an inverse correlation between PDS amplitude and X-ray luminosity seems to generally support the idea that less luminous objects have a smaller black hole mass (Lawrence & Papadakis 1993). On longer time scales, the PDS must flatten to low frequencies, or the total power would diverge.

As demonstrated by Vio et al. (1992), the PDS cannot be used to distinguish whether the process is linear or nonlinear. This determination is fundamental in AGN research, as it provides information about the structure of the emitting region. For example, one of the most widely accepted generic models to explain AGN variability, that the red noise power spectrum results from the flaring of many independent active regions, is an inherently linear model. If nonlinearity is discovered in the light curve, it means at least that the active regions must not be completely independent all the time, or in the extreme case, that there is a single emission region.

3C 390.3 is a luminous ($L_{X(2-10)} \sim 2 - 4 \times 10^{44}$ ergs s $^{-1}$) nearby ($z=0.057$) broad-line radio galaxy located in the North Ecliptic cap. It is well known as the prototypical source of broad double-peaked and variable $H\beta$ lines (e.g. Veilleux & Zheng 1991). 3C 390.3 is variable in all wave bands, including the optical (Barr et al. 1980) and UV (Zheng 1996), and it is a bright and variable X-ray source (see Eracleous, Halpern & Livio 1996 for a compilation).

During 1995, 3C 390.3 was subject to a monitoring campaign from radio through X-rays. Using the *ROSAT* HRI, we obtained the first well sampled X-ray light curve on time scales from days to months, shown in Figure 1. The surprising result is that there is clear evidence for nonlinear variability in the X-ray light curve, the first such reported for an AGN. This result imposes new constraints on AGN variability models. The details of the observations, the preliminary analysis of the *ROSAT* HRI data and the results from two *ASCA* observations made during the monitoring period are discussed in a companion paper Leighly et al. 1997a. The results from the optical, UV and radio monitoring will be reported elsewhere (Dietrich et al. 1997, O’Brien et al. 1997, Leighly et al. 1997b).

2. Variability Analysis

2.1. Evidence for Nonlinearity

The 3C 390.3 light curve looks different than X-ray light curves from AGN on shorter time scales (e.g. McHardy 1989). The most noticeable features are an isolated flare at about TJD 9800, and a series of flares starting at TJD 9960. Qualitatively speaking, such flares are evidence

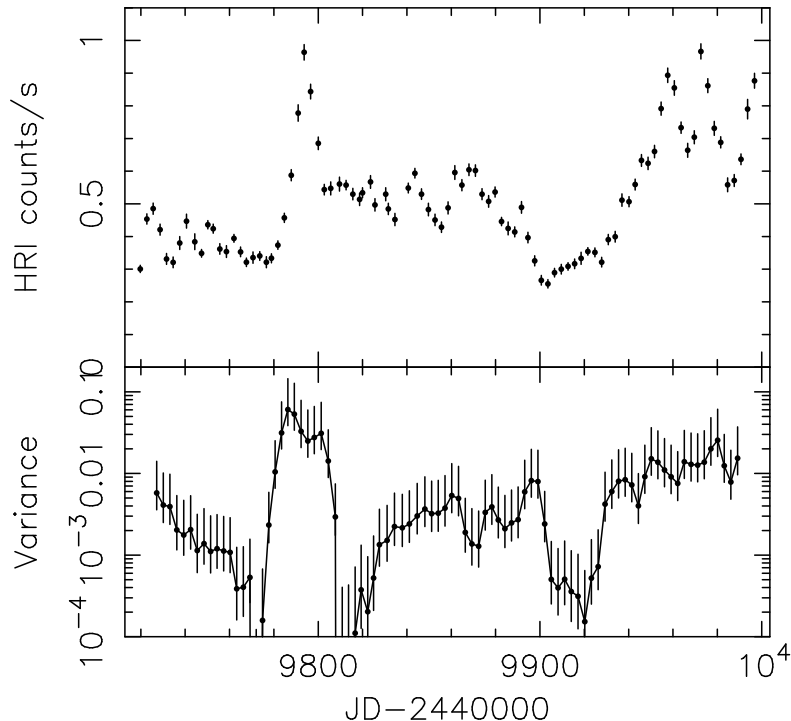


Fig. 1.— Top: *ROSAT* HRI light curve from monitoring observations of 3C 390.3; Bottom: Quiescent periods in the light curve can be detected by taking the variance over a sliding box with $N = 6$.

that the variability is nonlinear (e.g. Vio 1992).

Various statistical tests for nonlinearity are available. We use the method of Theiler et al. (1992), explained fully in this reference, which uses simulations to assess the significance of the detection of nonlinearity in the time series. First, a null hypothesis is conceived, and surrogate time series are simulated which have the properties of the null hypothesis. Then a nonlinear statistic is applied to the real time series and multiple realizations of the surrogate time series. If the value of the statistic for the real time series is significantly different than the distribution from the surrogate data, nonlinearity is detected, and the significance of the detection is the number of sigma difference between the real data values and mean of the surrogate values.

The null hypothesis that we chose is that the variability is linear but has a steep power density spectrum, as this is the here-to best model of AGN variability (e.g. Lawrence & Papadakis 1993). Surrogate data are generated by randomizing the Fourier phases but retaining the amplitudes of the discrete power spectrum obtained from the real data. Thus the surrogate data has the same power spectrum, circular autocorrelation, mean and variance as the real data, but has been linearized by the phase randomization. This takes advantage of the fact that the power spectrum measures only the linear properties, or the first two moments of the process (e.g. Vio et al. 1992);

thus linear and nonlinear time series can have the same power spectra.

Ideally, any nonlinear statistic can be used; however, some are more sensitive than others for our data. For example, the slope of the correlation integral is a useful statistic, since the asymptotic value is the dimension of the strange attractor (Grassberger & Procaccia 1983). However, after ignoring the first point and last four points of the light curve to reduce spurious high frequency components, there are only 88 points in our time series, and the slope of the correlation integral is noisy and not well defined. Instead, we use the value of the correlation integral $C(r)$ at a specific value of r (Theiler et al. 1992). The correlation integral counts the number of pairs of vectors with difference vector magnitude less than r ; this is generally larger for the optimal r_{in} if the process is nonlinear. For small r , the correlation becomes zero for larger dimensions, while for large r , the majority of pairs of vectors are counted, and since the observed and surrogate data are both normalized, the correlation integrals become indistinguishable. Figure 2, upper panel, shows the value of the correlation integral at $r_{in} = 0.5$ versus embedding dimension for the real data and for 10 realizations of the surrogate data. The lower panel of Figure 2 shows that the detection significance of the nonlinearity is $\gtrsim 6\sigma$ computed from 100 realizations of the surrogate data.

The detection of nonlinearity is corroborated by the presence of quiescent periods associated with intermittency in the light curve. Examination of the light curve shows that the variability before and after the flares seems to be reduced. Since the signal-to-noise of this time series is very high (~ 30), this can be quantified by computing the true variance over a sliding box (e.g. Isliker & Benz 1994) as shown in the lower panel of Figure 1.

2.2. The Variability Power Spectrum

Since the sampling is effectively even, the periodogram can be computed directly using the discrete Fourier transform. However, estimating power density spectrum (PDS) parameters is complicated by several problems. The time period spanned is short compared with the time scale of variability, so the value of average quantities can be estimated only poorly. Also, this light curve is clearly not stationary (see e.g. Papadakis & Lawrence 1995), so strictly speaking, the power density spectrum cannot be estimated from the periodogram. Furthermore, extensive simulations made by Papadakis & Lawrence (1995) demonstrate with few numbers of points, problems including red-noise leak of power toward high frequencies and aliasing toward low frequencies skew the periodogram severely.

The periodogram computed using the method of Papadakis & Lawrence (1993) is shown in the upper panel of Figure 3. A power law fit to the binned periodogram excluding the first and last points yields $s = 2.7$. Similar results are obtained if a spectral window is applied to the light curve ($s = 3.0$). This slope is much steeper than those found at higher frequencies using *EXOSAT*.

The structure function (SF) slope d is related to the slope of the power density spectrum by $s = 1 + d$ (e.g. Hughes, Aller & Aller 1992) again under the condition that the time series is

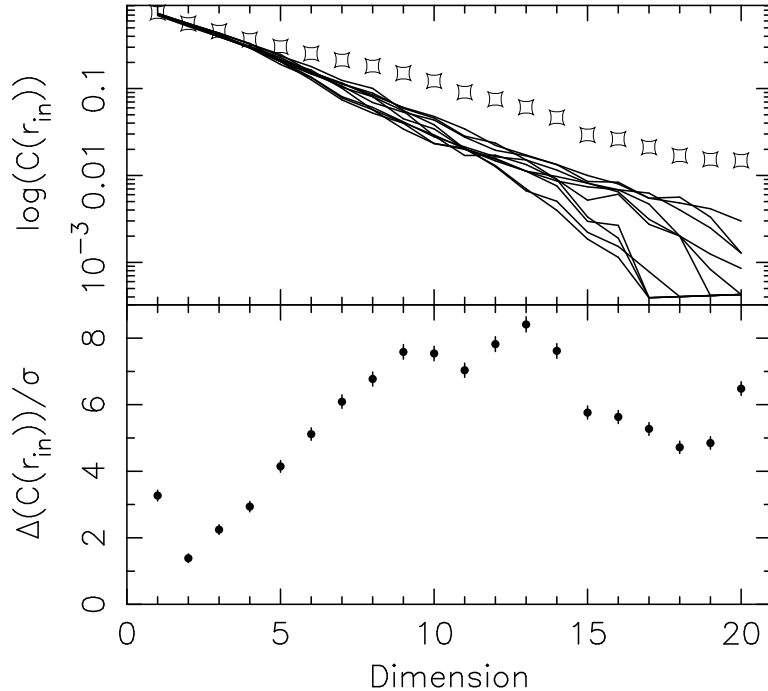


Fig. 2.— Detection of nonlinearity in the 3C 390.3 data, using the method of Theiler et al. 1992. Top: Squares show value of the correlation integral at $r_{in} = 0.5$ for the real data, while lines connect points from the simulated data; Bottom: Number of sigma difference between values from real data and mean of surrogate data.

stationary. The SF is shown in the lower panel of Figure 3. For lags between 6 and 64 days, the SF has a logarithmic slope of $d = 0.7$, corresponding to a PDS index of $s = 1.7$, close to the average high frequency slope of 1.55 found using *EXOSAT* data (Lawrence & Papadakis 1993). Simulating 1000 light curves with PDS index $s = 1.7$ and similar length, and fitting over the same interval gives mean $d = 0.58$ with standard deviation 0.27. Part of the difference between the periodogram and the structure function can be traced to the nonstationarity. The structure function slope ignores low frequencies, but the periodogram will be steepened by an overall trend in the data.

While information regarding the PDS is only poorly estimated using these data, note that the nonstationarity of the light curve could be evidence that the PDS has not turned over toward low frequencies indicating that the break in the power spectrum occurs on longer time scales than about 4 months for this comparatively luminous object. Alternatively, as nonlinear processes need not be intrinsically stationary, the power spectrum actually could be changing with time.

3. Discussion

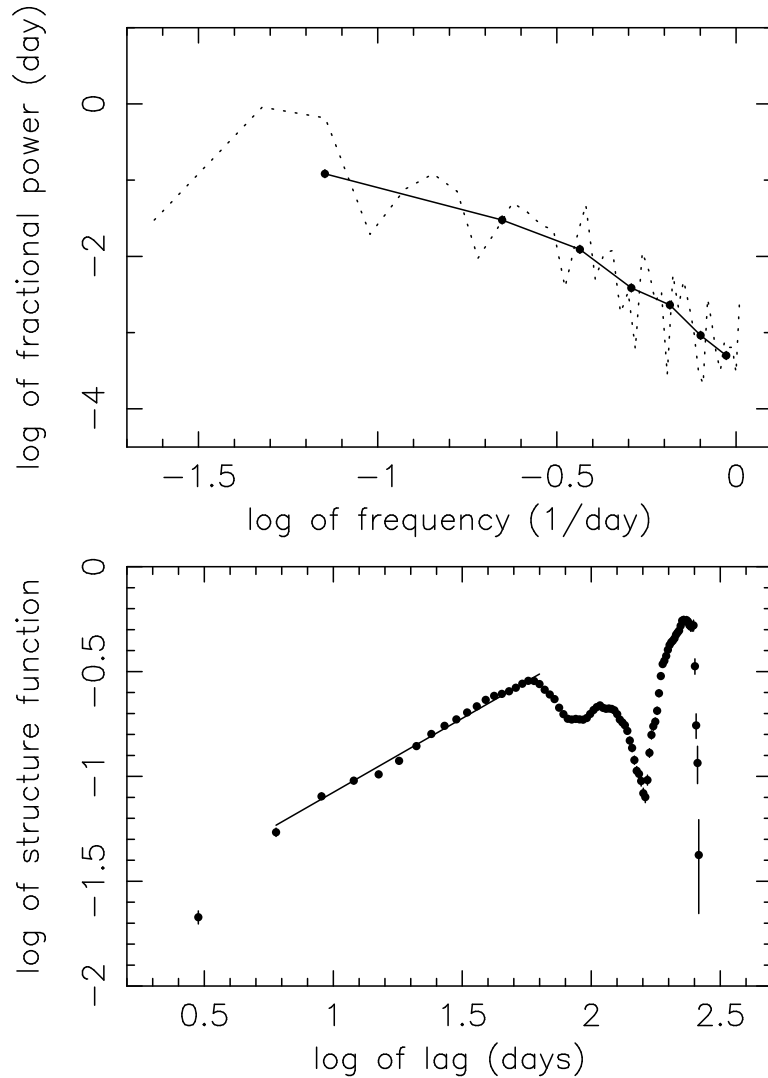


Fig. 3.— Top: the periodogram; Bottom: the structure function.

3.1. An X-ray jet in 3C 390.3?

3C 390.3 has a compact radio jet (Alef et al. 1996) and it is possible that the X-ray emission comes from the jet. If so, nonlinear X-ray variability may be expected since essentially a single emission region would be present. Furthermore, nonlinear variability has been found in the optical light curves from the OVV blazar 3C 345 (Vio et al. 1991).

However, there is spectral evidence that in 3C 390.3 the X-ray emission is predominantly isotropic. A broad iron $K\alpha$ line, similar to those found in radio-quiet Seyfert 1 galaxies (e.g. Fabian et al. 1995) has been detected in the X-ray spectrum (Eracleous, Halpern & Livio 1996). These broad iron lines are strong evidence for illumination of a relativistic accretion disk by the

X-ray source (Tanaka et al. 1995) and they are never seen in the X-ray spectra from blazars. Also, a weak X-ray reflection component, generally thought to be the signature of illumination of optically thick material by X-rays (e.g. George & Fabian 1991) has been observed in this object (Wozniak et al. 1997).

It is also possible that there are two highly variable X-ray emission components, one approximately isotropic with linear variability and the other from the jet, contributing superimposed flares. However, the reduction of variability in the quiescent periods before and after flares argues against this possibility.

3.2. Current X-ray Variability Models of AGN

Disk-corona models, in which the X-ray emission originates from comptonization of soft UV thermal photons in a corona of hot electrons lying above the disk, can successfully explain the UV– γ -ray broad band emission of radio-quiet AGN (e.g. Haardt & Maraschi 1993). To obtain the observed photon indices, γ -ray cutoffs and UV to X-ray ratios, the corona should not cover the disk completely, but rather be localized to a number of active blobs (Haardt, Maraschi & Ghisellini 1994). The X-ray variability would be stochastic if it is associated with variations in the number and luminosity of the independent active blobs. This situation can be modeled by shot noise, the sum of randomly occurring independent flares with perhaps variable exponential decay times, which can also explain the $1/f^s$ variability observed on time scales less than 1 day (e.g. Lawrence & Papadakis 1993). However, shot noise is a linear model, being simply a sum of independent events, and thus it cannot reproduce the light curve presented here. Similarly, a $1/f^s$ PDS can also be produced by the differential rotation of hot spots on a disk where the observed emission has been modified by gravitational effects (e.g. Bao & Abramowicz 1996), but again if the emission from each blob is independent, the variability should be linear.

3.3. Analogy with Cygnus X-1 and Reservoir Models

The Galactic black hole candidate Cyg X-1 in the low state has many similarities with radio-quiet AGN, including a $1/f^s$ power density spectrum. Recently, Negoro and collaborators have attempted to understand the variability of this object by identifying the largest flares in the light curves and stacking them to determine common properties. They find that the probability of flaring is significantly reduced before and after large flares (Negoro et al. 1995). The quiescence we observe before and after flares in the 3C 390.3 light curve seems to be a similar phenomenon.

A self-organized criticality (SOC) disk model was developed to explain these results (Mineshige, Ouchi, & Nishimori 1994). This model uses the concepts of self-organized criticality proposed by Bak et al. (1988) to explain $1/f$ variability observed in a wide variety of physical systems. The SOC accretion disk is comprised of numerous reservoirs. When a critical density

is reached in a reservoir, an unspecified instability is activated causing an avalanche of accretion and emptying of the reservoir. Adjacent reservoirs are coupled, so that triggering instability in one reservoir may result in instability in few or many adjacent reservoirs, resulting in a small or large flare. It is this coupling which provides the essential nonlinearity in the model. In this model, small flares occur randomly, since they originate from just a few reservoirs. Quiescent periods after large flares naturally occur while the large number of reservoirs emptied fill again. Quiescent periods before large flares happen because few or no small flares have occurred to release the accumulated potential energy. The predicted power density spectra are steep ($\propto 1/f^{1.6-1.8}$; Mineshige, Takekuchi & Nishimori 1994) similar to the estimate from the structure function found here, but also to the periodogram estimates from *EXOSAT* light curves (Lawrence & Papadakis 1993). A reservoir model has been discussed in the context of AGN by Begelman & De Kool (1990).

The analogy with 3C 390.3 may be quite direct. We note that the FWHM of the flare at TJD 9800 is roughly 12 days, while the typical FWHM of the shots in Cygnus X-1 is 0.2s (Negoro, Miyamoto & Kitamoto, 1994). The ratio of these timescales is $\sim 5 \times 10^6$. The mass of the black hole in Cygnus X-1 is thought to be about $10M_{\odot}$. If the flare time scale is directly proportional to the black hole mass, a mass of $\sim 5 \times 10^7 M_{\odot}$ would be implied, which is reasonable for this luminous object.

The authors thank the referee, Roberto Vio, for many useful comments especially regarding estimation of the PDS slope. K.M.L. thanks Chris Done, Tahir Yaqoob and Greg Madejski for useful discussions, and Randall A. LaViolette for pointing toward Theiler's method. K.M.L. gratefully acknowledges support by NASA grant NAG 5-2637 (ROSAT) and through a Science and Technology Agency postdoctoral fellowship.

REFERENCES

- Alef, W., Wu, S. Y., Preuss, E., Kellerman, K. I., & Qiu, Y. H. 1996, *A&A*, 308, 376
- Bak, P., Tang, C., Wiesenfeld, K. 1988, *Phys. Rev. A*, 38, 364
- Bao, G., & Abramowicz, M. A. 1996, *ApJ*, 465, 646
- Barr, P., et al. 1980, *MNRAS*, 193, 549
- Begelman, M. C., & De Kool, M. 1990, *Variability of Active Galactic Nuclei*, eds. H. R. Miller & P. J. Wiita (Cambridge: CUP) p. 198
- Dietrich, M., et al. 1997, in prep.
- Eracleous, M., Halpern, J. P., & Livio, M. 1996, *ApJ*, 459, 89
- Fabian, A. C., Nandra, K., Reynolds, C. S., Brandt, W. N., Otani, C., Tanaka, Y., Inoue, H., & Iwasawa, K. 1995, *MNRAS*, 277, L11
- George, I. M., & Fabian, A. C., 1991, *MNRAS*, 249, 352
- Grassberger, P., & Procaccia, I. 1983, *Physica*, 9D, 189
- Haardt, F., & Maraschi, L., 1993, *ApJ*, 413, 507
- Haardt, F., Maraschi, L., & Ghisellini, G. 1994, *ApJL*, 432, 95
- Hughes, P. A., Aller, H. D., & Aller, M. F. 1992, *ApJ*, 396, 469
- Islaker, H., & Benz, A. O. 1994, *A&A*, 285, 663
- Lawrence, A., & Papadakis, I. E., 1993, *ApJL*, 414, 85
- Leighly, K. M. et al. 1997a, accepted for publication in *ApJ*
- Leighly, K. M. et al. 1997b, in preparation
- McHardy, I. M. 1989, *Proc. 23rd ESLAB Symp.*, eds. J. Hunt and B. Battrock (Paris: ESA) p. 1111
- Mineshige, S., Ouchi, B., & Nishimori, H. 1994, *PASJ*, 46, 97
- Mineshige, S., Takekuchi, M., & Nishimori, H. 1994, *ApJL*, 435, 125
- Negoro, H., Miyamoto, S., & Kitamoto, S. 1994, *ApJL*, 423, 127
- Negoro, H., Kitamoto, S., Takekuchi, M., & Mineshige, S. 1995, *ApJL*, 452, 49
- O'Brien, P. T., et al. 1997, in prep.
- Papadakis, I. E., & Lawrence, A. 1993, *MNRAS*, 261, 612
- Papadakis, I. E., & Lawrence, A. 1995, *MNRAS*, 272, 161
- Tanaka, Y., et al. 1995, *Nature*, 375, 659
- Theiler, J., Eubank, S., Longtin, A., Galdrikian, B., & Farmer, J. D. 1992, *Physica*, D58, 77
- Veilleux, S. & Zheng, W. 1991, *ApJ*, 377, 89

Vio, R., Cristiani, S., Lessi, O., & Salvadori, L. 1991, ApJ, 380, 351

Vio, R., Cristiani, S., Lessi, O., & Provenzale, A. 1992, ApJ, 391, 518

Wozniak, P.R., Zdziarski A.A., Smith D., Madejski G.M. 1997, submitted to MNRAS

Zheng, W. 1996, AJ, 111, 1498